Am J Physiol Regul Integr Comp Physiol 297: R1570–R1581, 2009.
First published September 23, 2009; doi:10.1152/ajpregu.00430.2009.

Evolutionary structural and functional conservation of an ortholog of the GLUT2 glucose transporter gene (SLC2A2) in zebrafish

Juan Castillo,[1]* Diego Crespo,[1]* Encarnación Capilla,[1]* Mònica Díaz,[1] François Chauvigné,[2] Joan Cerdà,[2] and Josep V. Planas[1]*

[1]*Departament de Fisiologia, Facultat de Biologia, Universitat de Barcelona and Institut de Biomedicina de la Universitat de Barcelona, Barcelona, Spain; and* [2]*Laboratory Institut de Recerca i Tecnologia Agroalimentaries-Institute of Marine Sciences, Consejo Superior de Investigaciones Científicas, Barcelona, Spain*

Submitted 20 July 2009; accepted in final form 16 September 2009

Castillo J, Crespo D, Capilla E, Díaz M, Chauvigné F, Cerdà J, Planas JV. Evolutionary structural and functional conservation of an ortholog of the GLUT2 glucose transporter gene (SLC2A2) in zebrafish. *Am J Physiol Regul Integr Comp Physiol* 297: R1570–R1581, 2009. First published September 23, 2009; doi:10.1152/ajpregu.00430.2009.—In mammals, GLUT2 plays an essential role in glucose homeostasis. From an evolutionary perspective, relatively little is known about the biology of GLUT2, or other GLUTs, in nonmammalian vertebrates. Here, we have conducted studies to functionally characterize GLUT2 in zebrafish. First, we cloned the zebrafish ortholog of GLUT2 (zfGLUT2) encoding a protein of 504 amino acids with high-sequence identity to other known vertebrate GLUT2 proteins. The zfGLUT2 gene consists of 11 exons and 10 introns, spanning 20 kb and mapping to a region of chromosome 2 that exhibits conserved synteny with human chromosome 3. When expressed in *Xenopus* oocytes, zfGLUT2 transported 2-deoxyglucose (2-DG) with similar affinity than mammalian GLUT2 (K_m of 11 mM). Transport of 2-DG was competed mostly by D-fructose and D-mannose and was inhibited by cytochalasin B. During early development, zfGLUT2 expression was detected already at 10 h postfertilization and remained elevated in 5-day larvae, when it was clearly localized to the liver and intestinal bulb. In the adult, zfGLUT2 expression was highest in testis, brain, skin, kidney, and intestine, followed by liver and muscle. In the intestine, zfGLUT2 transcripts were detected in absorptive enterocytes, and its mRNA levels were altered by fasting and refeeding, suggesting that its expression in the intestine may be regulated by the nutritional status. These results indicate that the structure and function of GLUT2 has been remarkably well conserved during vertebrate evolution and open the way for the use of zebrafish as a model species in which to study the biology and pathophysiology of GLUT2.

gene expression; glucose transport; affinity; intestine

GLUCOSE CAN ENTER THE CELLS by facilitated diffusion mediated by a large family of glucose transporter proteins (GLUTs) comprising 14 different members. GLUTs are integral membrane proteins that contain 12 membrane-spanning helices with both the amino and carboxyl termini exposed to the cytosol. Each glucose transporter isoform plays a specific role in glucose metabolism as determined by its pattern of tissue expression, substrate specificity, transport kinetics, and regulated expression under different physiological conditions (45). Among the known class I GLUT isoforms (GLUT1, 2, 3, and 4), GLUT2 has been shown in mammals to be expressed in a variety of different tissues, predominantly in the liver, pancreas, small intestine, and kidney and was initially referred to as the liver-type GLUT (42). Functionally, GLUT2 transports sugars (glucose, fructose, mannose, and galactose) with low affinity but has also been shown to be a high-affinity glucosamine transporter (44). As a class I GLUT, GLUT2 is unique in its ability to transport both D-glucose and D-fructose (4, 6, 27), a feature attributed to the lack of the QLS motif in transmembrane (TM) domain 7. From a physiological point of view, GLUT2 is known to play in mammals an important role in a number of different processes. These include the intestinal and renal absorption of glucose, the stimulation of insulin secretion by glucose in pancreatic β-cells, the entry and output of glucose by the liver, and the glucosensing capability of specific brain regions involved in the regulation of glucose metabolism and food intake (45). In the intestine, GLUT2 is expressed in the brush-border and basolateral membranes, and metabolic and endocrine factors regulate GLUT2 mRNA levels, as well as the distribution of GLUT2 molecules to the apical membrane (3, 8, 19, 20). However, the precise physiological role of GLUT2 is far from understood. The notion that GLUT2 was mediating the exit of glucose from the intestinal enterocyte to the circulation, one of the most widely accepted functions of GLUT2, has been questioned by the findings that mice lacking a functional GLUT2 gene and humans with a mutation in the GLUT2 gene do not appear to have any defect in intestinal glucose absorption (41).

Among nonmammalian vertebrates, GLUT2 has been to date identified and studied at the molecular level in avian and fish species (15, 22, 38, 49). In fish, recent studies have shown that the expression of GLUT2 in pancreatic cells, as well as in the hypothalamus, appears to be regulated by hormonal and metabolic signals (31), whereas the hepatic expression of GLUT2 is not affected by fasting and/or refeeding (15, 30). The regulation of the expression of GLUT2 in the intestine, however, has not been examined to date in fish. Importantly, the biochemical and functional characteristics of GLUT2 are not known in any nonmammalian vertebrate. To improve our understanding of the biology of GLUT2, we set out to identify the GLUT2 gene in the zebrafish (*Danio rerio*) and study its expression from early embryonic life into adulthood, as well as its specific transport properties. The zebrafish is growing in importance as a model organism for physiological and pharmacological studies and even human disease modeling (2, 26, 35) and, therefore, could be a useful animal model species in which to study the function and regulation of GLUT2. The results from our study indicate that zebrafish express a true GLUT2 ortholog with similar structure and sugar transport properties as mammalian GLUT2 that is expressed early in

* These authors contributed equally to this study.
J. V. Planas, Departament de Fisiologia, Facultat de Biologia, IBUB, Universitat de Barcelona, Av. Diagonal 645, 08028 Barcelona, Spain (e-mail: jplanas@ub.edu).

development and that shows a characteristic pattern of expression in adult tissues. Furthermore, the expression of GLUT2 in the intestine is altered by fasting and refeeding.

MATERIALS AND METHODS

Animals. Zebrafish (*Danio rerio*) were reared at 28.5°C under a 12:12-h light-dark cycle at the University of Barcelona. Zebrafish embryos were incubated in embryo medium, and their development was examined under a microscope according to the staging series (21). Zebrafish embryos and larvae for RNA extraction were frozen directly in liquid nitrogen and stored at −80°C until use. To collect tissues from adult animals, fish were killed by an excess of anesthesia using 3-aminobenzoic acid ethyl ester (0.1 g/l; Sigma-Aldrich, Alcobendas, Spain), tissues were quickly removed, frozen in liquid nitrogen and stored at −80°C until processed for RNA extraction.

For the nutritional study, adult zebrafish were separated into two groups: one group of fish ($n = 6$) was fed with flake food each day at the same time, while the other group ($n = 12$) was deprived of food. Each group of fish was placed in a separate tank with an independent water pump and filter recirculating system. After 15 days of fasting, six fish from the fasted group and all the fish from the fed group were killed as described above. The remaining six fish from the fasted group were refed for 6 days. Blood samples were obtained by caudal section in anesthetized animals and, because of the low volume of blood, samples from all individuals ($n = 6$) of each group (fed, fasted, and refed) were pooled. Blood was centrifuged at 1,500 rpm for 10 min, and plasma glucose levels were determined using a commercial kit (Spinreact, Girona, Spain). The experimental protocols used in this study have been reviewed and approved by the Ethics and Animal Welfare Committee of the University of Barcelona, Spain.

Cloning of zebrafish GLUT2. The zebrafish GLUT2 cDNA was cloned from a whole-body zebrafish cDNA library (ZAP Express, Stratagene, La Jolla, CA; kindly donated by Dr. Frederick W. Goetz) by screening at high stringency using as a probe I.M.A.G.E. Consortium CloneID fb79d10 (25) with homology to human GLUT2. After three rounds of screening by plate hybridization, two positive clones were obtained. Once purified to homogeneity, clones were digested with *Eco*RI and *Xho*I to determine the insert size. Both clones were ~2.5 kb in length and, when sequenced using the BigDye terminator cycle sequencing kit (PE Biosystems, Foster City, CA) and an ABI Prism 360 sequencer, were found to be identical and represent the same cDNA. Sequence compilations, comparisons, and features were obtained using the Wisconsin package version 11.0 (Genetics Computer Group). The assembled full-length zebrafish GLUT2 cDNA sequence was entered in GenBank with accession number DQ098687.

The zebrafish GLUT2 gene was cloned in silico by comparing the full-length zebrafish GLUT2 cDNA sequence to the zebrafish genome sequences at the Ensembl Genome Browser (http://www.ensembl.org/Danio_rerio/index.html) using the BLAST algorithm. A 20-kb genomic sequence (ZFISH7:2:21467945:21487811), mapped to chromosome 2, was found to contain the entire genomic structure of the zebrafish GLUT2 gene, with the exception of the promoter region.

Sequence analysis. Sequence data were compiled from the National Center for Biotechnology Information (NCBI, Bethesda, MD, USA). Alignments were performed using Bioedit Sequence Alignment Editor (16), which uses the CLUSTAL W algorithm (40). Isoelectrical point and molecular mass were predicted using the Expasy Proteomics server of the Swiss Institute of Bioinformatics (SIB) (http://www.expasy.ch/cgi-bin/pi_tool) (12). For phylogenetic analysis, alignments were imported into *MEGA* version 3.1 (24). Phylogenetic trees were constructed using the neighbor-joining (NJ) method (33) with Poisson correction. Bootstrap analysis was performed with 10,000 replicates. Exon-intron boundaries in the zfGLUT2 gene were identified by aligning the cDNA and genomic sequences of zfGLUT2 using the Spidey software (http://www.ncbi.nlm.nih.gov/spidey/). The gene order of the human GLUT2 locus in chromosome 3 and that of the zfGLUT2 locus in chromosome 2 was obtained from Ensembl release version 53.

Analysis of the expression of zfGLUT2. Total RNA from larval and adult zebrafish tissues was isolated using Tri Reagent (Molecular Research Center, Cincinnati, OH) following the manufacturer's instructions. For zebrafish embryos, the chorion was removed with forceps, and total RNA was isolated using the same procedure. Total RNA (2.5–5 μg) was reverse transcribed with Superscript III reverse transcriptase (Invitrogen, Barcelona, Spain) and conventional PCR reactions were performed using *Taq* DNA polymerase (Biotools, Madrid, Spain) with 2 mM $MgCl_2$, 800 nM primer final concentration and 1 μl of reverse-transcribed cDNA. The cycling conditions were 94°C for 5 min followed by 25 cycles of 94°C for 40 s, 50°C for 50 s and 72°C for 50 s, and a final extension step at 72°C for 10 min. The reactions were run on 1% agarose gels and stained with ethidium bromide. Parallel RT-PCR reactions were carried out with specific primers against a conserved region of the 18S rRNA as a control. The sequences of all the primers used in gene expression analysis are shown in Table 1. Quantitative real-time PCR analysis was performed using a MyiQ thermocycler and the SYBR Green PCR Mix (Bio-Rad, Hercules, CA). Results were evaluated with the iCycler IQ real-time detection system software (Bio-Rad). Total volume (20 μl) of reactions contained 500 nM of each amplification primer, 10 μl of 2× SYBR Green PCR Mix and 5 μl of a 1:100 dilution of cDNA (1:1,000 for determination of 18S). The real-time PCR analysis consisted of 1 cycle of 95°C for 5 min, 40 cycles of 95°C for 10 s, and 60°C for 30 s, 1 cycle of 95°C for 1 min, 1 cycle of 55°C for 1 min, followed by a melting curve from 55°C to 95°C, with 0.5°C increments every 10 s. All quantifications were normalized to the endogenous control 18S rRNA, and its expression levels did not vary among the different conditions examined (data not shown).

Generation of RNA probes for in situ hybridization. The pattern of expression of zfGLUT2 in embryos and adult tissues was also analyzed by in situ hybridization (ISH) using digoxigenin-labeled sense and antisense RNA probes encompassing the full-length zfGLUT2 cDNA. RNA probes were generated by in vitro transcription of 1 μg of zfGLUT2 linearized DNA template using T3 or T7 RNA polymerase (Roche Diagnostics, Mannheim, Germany), according to the orientation of the insert. Linearized probes were precipitated with LiCl/ethanol, dissolved in diethylpyrocarbonate-treated water, and stored at −80°C until use, following the manufacturer's recommendations (Roche). Sense-strand probe was used as specificity control for hybridization and revealed no signal.

Whole-mount ISH. Embryos were collected, carefully dechorionated with forceps, allowed to develop at 28.5°C until the appropriate stage, and then fixed by incubation overnight in 4% paraformaldehyde (PFA) at 4°C. Embryos older than 24 hours post fertilization (hpf) were incubated in 3% H_2O_2 with 0.5% KOH to prevent accumulation of pigment as previously reported (39). After fixation, embryos were dehydrated and stored at −20°C in 100% methanol prior to ISH. Whole-mount embryos were rehydrated, washed in PBS-T (1 M Na_2HPO_4, 1 M NaH_2PO_4, 1.5 M NaCl, pH 7.4 containing 0.1%

Table 1. *Sequences of primers used in gene expression analyses*

Primer	DNA Sequence	Direction	Size of Amplicon
GLUT2F	5′-TTATCTACTTCCGTGTACC-3′	Forward	334 bp
GLUT2R	5′-GCACCATCTTCCACAATTATC-3′	Reverse	
GLUT2 real-timeF	5′-CCACCGAAAACATGGAGGAGTT-3′	Forward	167 bp
GLUT2 real-timeR	5′-TGTCATAACACCTGGGCTCTGTG-3′	Reverse	
18SF	5′-CGAGCAATAACACGTCTGTG-3′	Forward	211 bp
18SR	5′-GGGCAGGGACTTAATCAA-3′	Reverse	

Tween 20), and digested with proteinase K (Sigma; 1 μl/ml in PBS-T). The reaction was then blocked with a stop-solution containing 2 mg/ml glycine in PBS-T. After two washes with PBS-T, the sections were postfixed with 4% PFA in PBS-T for 20 min. Prehybridization with hybridization solution consisting of 50 μg/ml heparin, 100 μg/ml calf thymus DNA, 50% formamide, 0.1% Tween 20, and 5× SSC (0.15 M NaCl, 0.05 M sodium citrate, pH 7) was carried out for 1 h at 55°C. Hybridization was performed overnight at 55°C with the riboprobe diluted at 1:300 in hybridization solution. The embryos were rinsed with PBS-T and washing solution (50% formamide, 0.1% Tween 20, 5× SSC in distilled water) at 55°C and then incubated with anti-digoxigenin-AP antibody (Roche; diluted 1:2,000 in PBS-T) for 1.5 h at room temperature. After washing with PBS-T and AP buffer (100 mM NaCl, 50 mM $MgCl_2$, 100 mM Tris-HCl pH 9.5), the embryos were incubated in a 5-bromo-4-chloro-3-indolyl phosphate/nitro blue tetrazolium liquid-substrate system (BCIP/NBT, Roche). The staining reaction was monitored under a dissecting microscope and was stopped when appropriate with PBS-T at room temperature. Embryos were then mounted under a coverslip in 87% glycerol prior to observation under microscope (Leica, model DM LB).

ISH on frozen sections. Following overnight fixation in 4% PFA at 4°C, zebrafish tissues were equilibrated in 15% sucrose in PBS until the tissues sank. Tissues then were embedded in fresh Tissue-Tek OCT (Sakura Zoeterwoude, The Netherlands) and frozen in an ethanol/dry ice bath. ISH was carried out on 17-μm tissue sections cut using a Leica cryostat. Hybridization with the riboprobes (concentration of 1:300–1:500) was performed overnight in hybridization buffer (1× salts, 50% deionized formamide, 10% dextran sulfate, 1 mg/ml yeast tRNA, 1× Denhardt's) at 55°C in a humidified chamber (1× salts/50% formamide). Coverslips were removed by washing in 2× SSC at 45°C, then the slides were washed for 30 min with increasing stringency (2× SSC, 1× SSC, 0.5× SSC) at 45°C and subsequently incubated with RNase A (Sigma; 10 μg/ml) in sodium chloride-Tris-EDTA (STE) buffer (10 mM Tris-HCl, pH 8, 10 mM EDTA, 100 mM NaCl) for 40 min at 37°C. Finally, the slides were washed for 1 h with Tris-buffered saline-Tween (TBS-T) (150 mM NaCl, 10 mM KCl, 50 mM Tris-HCl pH 7.5, 0.1% Tween 20) at room temperature, and blocking was performed with 20% inactivated lamb serum (Gibco)/2% blocking reagent (Roche) in TBS-T. The staining procedure was performed with anti-digoxigenin-AP (4 h to overnight at room temperature) by using BCIP/NBT system (Roche Diagnostics, Mannheim, Germany) and stopped with PBS-T. Then the slides were air dried, mounted using aqueous mounting medium (glycerol 87%), and observed with a Leica microscope.

Uptake of 2-deoxy-D-glucose by zfGLUT2 in Xenopus oocytes. The zfGLUT2 construct for heterologous expression in *Xenopus laevis* oocytes was generated by subcloning the full-length zfGLUT2 cDNA into the pSP64T vector (23). Since this vector contains a unique BglII cloning site to allow the gene of interest to be flanked by the 5′ and 3′ untranslated regions of the *Xenopus* β-globin gene, compatible BclI sites were first introduced by PCR comprising nucleotides 1 to 1,560 of zfGLUT2. Subsequently, capped RNA (cRNA) for microinjection was synthesized with SP6 RNA polymerase from the EcoRI-linearized pSP64T-zfGLUT2 construct. Isolation, microinjection (10 ng of cRNA per oocyte) and defolliculation of stages V and VI oocytes were performed as previously described (34). On *day 3*, groups of 10 healthy oocytes per condition (uninjected control and zfGLUT2-injected) were selected for glucose uptake assays using the radiolabeled glucose analog 2-deoxy-D-[2,6-^{3}H]glucose (2-[^{3}H]DG; 46.0 Ci/mmol specific activity; GE Healthcare, Segovia, Spain). Experiments on zero-*trans* kinetics, cytochalasin B inhibition, and substrate specificity were performed at room temperature under subtle agitation exactly as previously described for the salmon GLUT4 transporter (7). For each experiment, the specific 2-DG uptake mediated by zfGLUT2 was calculated by subtracting the average uptake value obtained for the noninjected oocytes. For the substrate specificity and cytochalasin B inhibition experiments, data are presented as a percentage over the control group (without competitor or inhibitor) (8–10 oocytes per group from two to three independent experiments). For the kinetic experiments (7–10 oocytes per group in four independent experiments), linearizations and affinity constant (*Km*) calculations were performed using the Prism 3.0 package.

Statistical analysis. Results are presented as means ± SE. Statistical differences between conditions were analyzed by one-way ANOVA followed by Tukey's post hoc test. Differences were considered statistically significant at $P < 0.05$.

RESULTS

The zebrafish genome contains and expresses an ortholog of human GLUT2. A zebrafish whole body cDNA library was screened with a zebrafish cDNA clone with high homology to mammalian GLUT2, and several positive clones were obtained after three high-stringency rounds. The resulting full-length cDNA sequence was 2,722 bp long and contained a 33-bp 5′ UTR region, a 1,515 bp ORF and a 1,174 bp 3′ UTR region, which included the poly(A) tail. The deduced amino acid sequence corresponded to a protein of 504 amino acids (Fig. 1), with a predicted molecular mass of 54.7 kDa and an isoelectric point of 8.71. This putative protein showed the highest sequence identity to other cloned fish GLUT2 sequences (72%, 74%, and 75% to sea bass, Atlantic cod, and rainbow trout) and lower sequence identity to amphibian (62% to *Xenopus*), avian (64% to chicken), and mammalian (~58%) GLUT2 sequences. Furthermore, the deduced zebrafish protein had only 54% sequence identity to zebrafish GLUT1 and, compared with human class I GLUT sequences, it showed 55%, 58%, 49%, and 56% sequence identity to human GLUT1, GLUT2, GLUT3, and GLUT4, respectively. Phylogenetic analysis to determine the degree of relatedness of the putative zebrafish protein to vertebrate class I GLUT proteins clearly showed that it clustered with fish GLUT2 sequences and that these were more similar to other vertebrate GLUT2 sequences than to any other GLUT isoforms (Fig. 2). Therefore, the deduced zebrafish protein sequence was considered the zebrafish ortholog of GLUT2 and was named zebrafish GLUT2 (zfGLUT2). Alignment of the amino acid sequences of zfGLUT2, Atlantic cod GLUT2, rainbow trout GLUT2 and human GLUT2 revealed a high degree of structural conservation among the various fish and human GLUT2 proteins (Fig. 1), evidencing the typical 12 TM structure of facilitated glucose transporters, as well as specific functional characteristic motifs of GLUT2 proteins (see DISCUSSION). The nucleotide sequence of the full-length zebrafish GLUT2 cDNA was deposited in GenBank under accession number DQ098687.

A single zfGLUT2 gene (ENSDARG00000056196) was identified in silico in the zebrafish genome sequence database and consisted of 11 exons and 10 introns spanning ~20 kb, mapping to chromosome 2 (Fig. 3, *A* and *D*). The translation initiation codon ATG and the termination codon TGA were located in exons 1 and 11, respectively. The gene structure of zfGLUT2, including the size and location of individual exons and introns within the zfGLUT2 gene, was determined by comparing the zfGLUT2 cDNA sequence with the zebrafish genome sequence (Table 2). All exon-intron boundaries contained the consensus 5′- and 3′-splice donor and acceptor sequences, respectively. We detected only one base difference in the coding region of the zfGLUT2 gene with respect to the zfGLUT2 cDNA sequence cloned in the present study: the

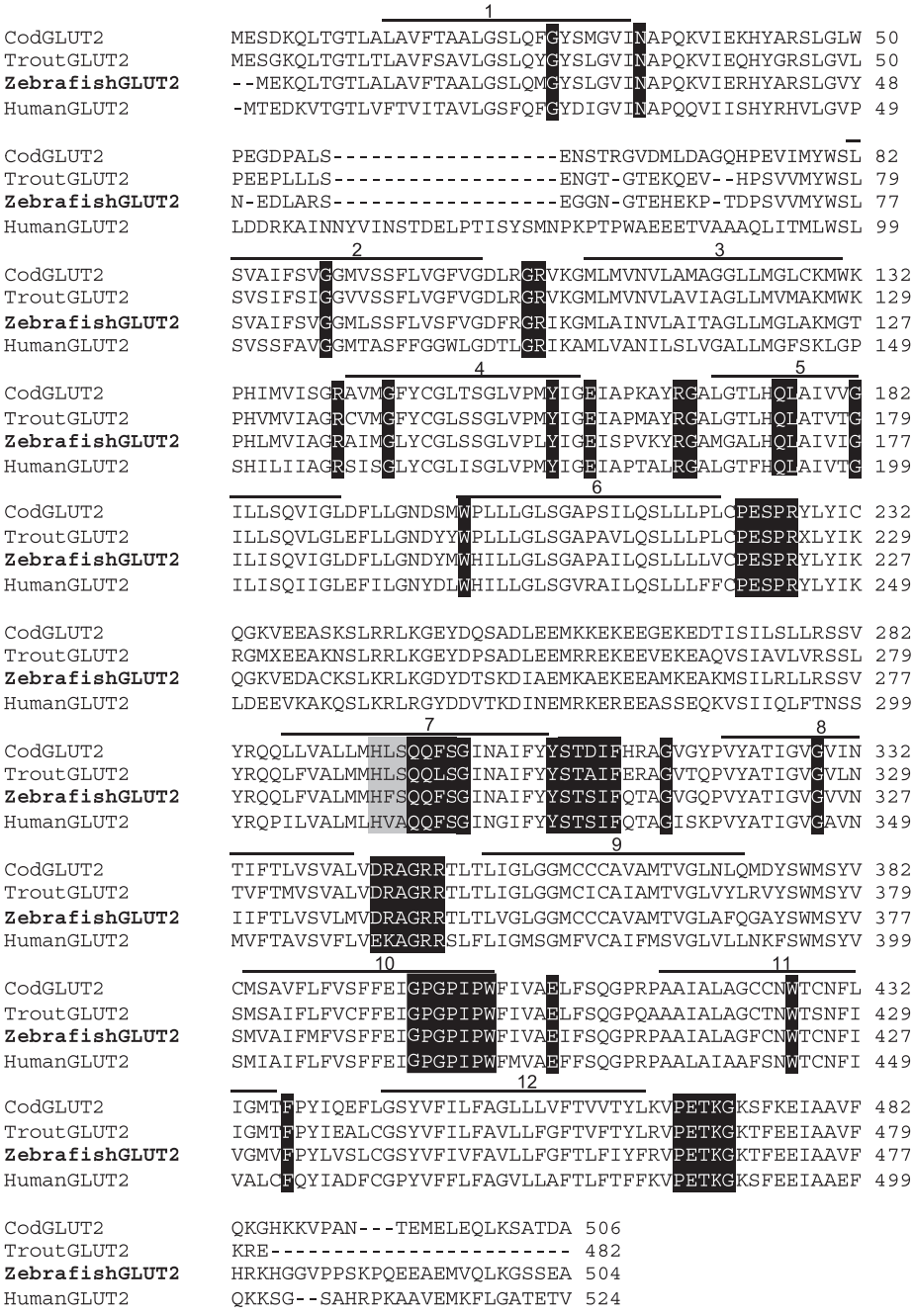

Fig. 1. Amino acid alignment of zebrafish GLUT2 with other fish GLUT2 sequences (trout and cod) and human GLUT2. Gaps in the amino acid sequences are indicated with a dash (-). SwissProt accession numbers for human, trout, and Atlantic cod GLUT2 are AAA59514, AAK09377, and AAV63984, respectively. Amino acids are represented by the single letter code, and numbering corresponds to rainbow trout GLUT2 residues. Lines with Arabic numbers indicate the 12 TM domains. The predicted N-glycosylation site and other important conserved motifs, such as those corresponding to specific sugar transporter signatures, as well as those involved in glucose specificity of class I glucose transporters are shown highlighted in black. The HVA motif characteristic of mammalian GLUT2 is highlighted in gray.

codon for Phe^{431} in exon 10 was GTT instead of TTT, which was translated into Val. We determined the synteny between the human GLUT2 and the zfGLUT2 genes by identifying genes flanking the GLUT2 loci in the human and zebrafish genomes (Fig. 3*C*). Analysis of these loci identified several zebrafish genes in chromosome 2 (GHSR, PLD1, TNKA, EIF5A2, and SLC7A1) with orthologs on human chromosome 3 (Fig. 3*B*), showing that in this genomic region, the gene order (GHSR, PLD1, TNKA, SLC2A2, EIF5A2, and SLC7A14) has been remarkably well conserved since the divergence of fish and mammals. The conserved synteny observed strongly supports the classification of zfGLUT2 as an ortholog of the human GLUT2 gene.

zfGLUT2 is expressed early during development in zebrafish. To describe the pattern of expression of zfGLUT2 during zebrafish development, we studied the expression of zfGLUT2 at regular intervals from 4 hpf until the larval stage, which is reached approximately at 4–5 days postfertilization (dpf). Gene expression was analyzed by conventional RT-PCR (Fig. 4*A*), quantitative real-time PCR (Fig. 4*B*) and also by whole-mount ISH (Fig. 5). Quantitative analysis of zfGLUT2 expression revealed very low levels of expression at the beginning of embryonic development (4–8 hpf; late blastula stage) that increase significantly at 10 hpf (end of gastrulation) and subsequently decrease at 24 hpf. At 36 hpf, zfGLUT2 expression levels progressively increase until the larval stage,

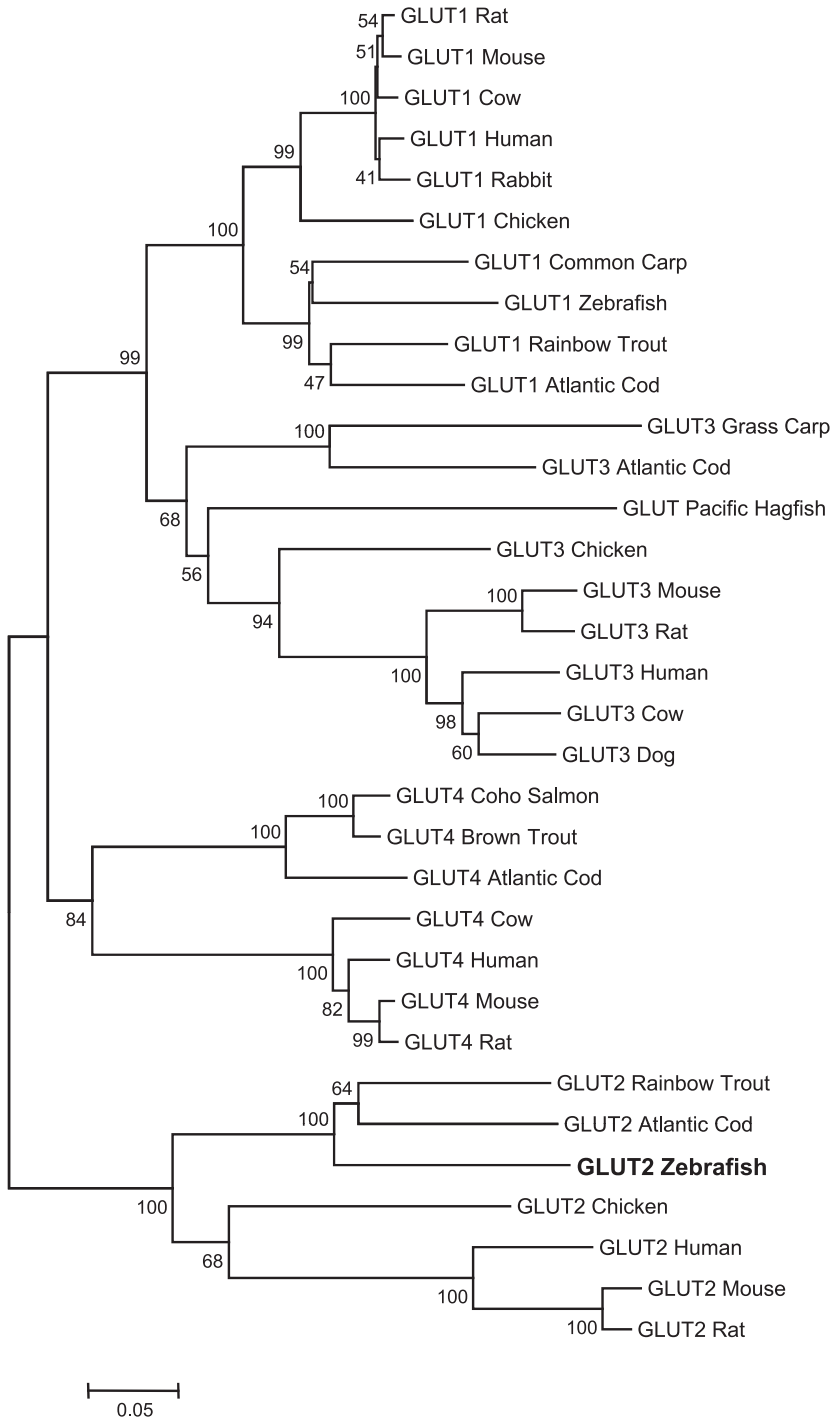

Fig. 2. Phylogenetic tree of known vertebrate GLUT protein sequences. A phylogenetic tree was constructed with the complete protein sequence of zebrafish GLUT2, and a number of protein sequences corresponding to various vertebrate GLUTs. SwissProt accession numbers: GLUT1 common carp (AAF75683), GLUT1 rainbow trout (AAF75681), GLUT1 Atlantic cod (AAS17880), GLUT1 chicken (AAB02037), GLUT1 human (AAA52571), GLUT1 rabbit (P13355), GLUT1 cow (P27674), GLUT1 rat (P11167), GLUT1 mouse (AAA37752), GLUT2 chicken (Q90592), GLUT2 rainbow trout (AAK09377), GLUT2 zebrafish (AAZ43092), GLUT2 human (AAA59514), GLUT2 mouse (P14246), GLUT2 rat (P12336), GLUT2 Atlantic cod (AAV63984), GLUT3 cow (AAK70222), GLUT3 dog (P47842), GLUT3 human (AAB61083), GLUT3 mouse (AAH34122), GLUT3 rat (Q07647), GLUT3 chicken (AAA48662), GLUT3 grass carp (AAP03065), GLUT3 Atlantic cod (AAT67456), GLUT4 cow (Q27994), GLUT4 human (AAA59189), GLUT4 mouse (P14142), GLUT4 rat (P19357), GLUT4 coho salmon (AAM22227), GLUT4 brown trout (AAG12191), GLUT4 Atlantic cod (AAZ15731), and Pacific hagfish (AAL27090). The tree was constructed as described in Materials and Methods. The scale bar represents the number of substitutions per amino acid site. Numbers above nodes indicate bootstrap proportions (10,000 replicates).

with a nonsignificant decrease in expression at 48 hpf (Fig. 4*B*). The highest levels of expression of zfGLUT2 during early development were observed at 72 hpf (hatching) and at 5 dpf (120 hpf; onset of exogenous feeding).

Whole-mount ISH of zebrafish embryos revealed that zfGLUT2 expression is localized ubiquitously throughout the embryo at 10 hpf (Fig. 5). At 24 hpf, zfGLUT2 expression is strongly detected in the yolk syncytial layer (YSL) followed by the developing intestine (Fig. 5, *D* and *E*). At 72 hpf, zfGLUT2 transcripts were clearly detected in liver and were weakly observed in the YSL (Fig. 5, *G* and *H*). The liver continued to express zfGLUT2 mRNA at 5 dpf. At this stage, zfGLUT2 expression was also detected in the anterior intestine (intestinal bulb) (Fig. 5, *J* and *K*). Negative controls with the sense-strand probe gave no signal (Fig. 5, *A*, *C*, *F*, *I*).

The expression of zfGLUT2 is widely distributed in adult tissues and identified in liver and intestinal cells. The presence and the level of zfGLUT2 expression in adult zebrafish tissues were examined by conventional RT-PCR, quantitative real-time PCR, and ISH on frozen sections. Using specific zfGLUT2 primers, we have detected the expression of zfGLUT2 in all the zebrafish tissues studied (Fig. 6*A*). Quan-

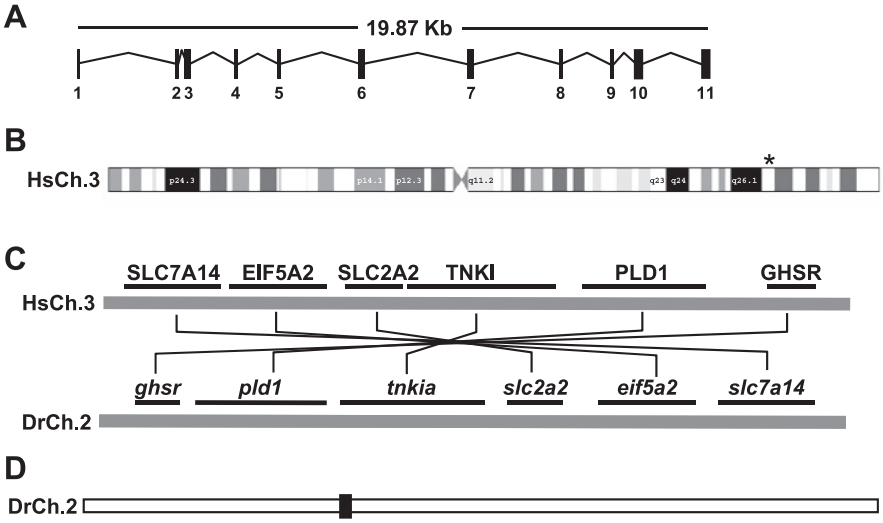

Fig. 3. Genomic structure and chromosomal localization of the zebrafish GLUT2 (*slc2a2*) gene and its human ortholog. *A*: organization of the zebrafish GLUT2 gene. Exons are numbered and indicated by the black boxes and introns are indicated by lines. *B*: position of the genomic region containing the human GLUT2 gene (indicated by an asterisk) in human chromosome 3 (HsCh.3). *C*: conserved synteny in the regions containing the GLUT2 gene in HsCh.3 and zebrafish chromosome 2 (DrCh.2). Surrounding *slc2a2*, the genes *ghsr* (ghrelin receptor), *pld1* (phospholipase D1), *tnika* (TRAF2 and NCK-interacting protein kinase), *eif5a2* (eukaryotic translation initiation factor 5A-2), and *slc7a14* (probable cationic amino acid transporter) appeared arranged in the same order in HsCh.3 and DrCh.2. *D*: localization of the zebrafish GLUT2 gene in chromosome 2, as indicated by a box.

tification of the relative expression levels of zfGLUT2 by real-time PCR revealed that zfGLUT2 expression is highest in testis, brain, skin, kidney, and intestine, followed by liver and muscle (Fig. 6*B*). Moreover, zfGLUT2 expression is very low in gills, eyes, ovary, and heart.

ISH on frozen sections revealed the presence of zfGLUT2 transcripts in intestine and liver (Fig. 7). In the intestine, zfGLUT2 is expressed in the absorptive enterocytes and in the mesenchyme, both in the lamina propria and the muscularis layer; however, no apparent expression of zfGLUT2 is detected in the goblet cells (Fig. 7*B*). In the liver, zfGLUT2 mRNA is expressed ubiquitously throughout the tissue (Fig. 7*D*). The expression of zfGLUT2 in the zebrafish brain was also studied, but we were unable to detect any signal (data not shown). In the intestine and liver, negative controls with the sense-strand probe gave no signal (Fig. 7, *A* and *C*).

zfGLUT2 has similar sugar transport properties than mammalian GLUT2. To functionally characterize the zfGLUT2 transporter, we used the *Xenopus laevis* oocyte heterologous expression system. *Xenopus* oocytes expressing zfGLUT2 transported 2-DG in a dose- and time-dependent manner (data not shown), providing the first evidence that zfGLUT2 may be a functional glucose transporter. First, to characterize the ability of zfGLUT2 to transport 2-DG, a series of zero-*trans* kinetics experiments with 2-DG were performed. The Lineweaver-Burk linearization plot from all the experiments combined is shown in Fig. 8*A*. The K_m value (obtained as equal to $-1/\times$ intercept) for the zfGLUT2 transporter was 11 mM with an R^2 value of 0.9901. In the inset, the K_m values from all four independent experiments are shown. Second, substrate specificity and cytochalasin B inhibition experiments were performed. From preliminary experiments, uptake conditions were settled for these experiments to ensure linearity (50 μM 2-DG final concentration, 30 min). Under these conditions, and in the absence of inhibitor and/or competitor (control conditions), zfGLUT2 transported 2-DG at a rate of 3.35 ± 0.29 pmol of glucose per min per oocyte, depending on the batch of oocytes used. Uptake of 2-DG by zfGLUT2-expressing oocytes was significantly inhibited in a concentration dependent manner by cytochalasin B, a specific inhibitor of facilitative transporters (Fig. 8*B*). To test the substrate specificity of the zfGLUT2 transporter, 2-DG uptake was performed in the presence of other sugars at a final concentration of 50 mM (Fig. 8*C*). zfGLUT2-mediated 2-DG transport was significantly competed ($P < 0.05$) by D-glucose and D-mannose, followed by D-fructose. D-galactose, and L-glucose were also able to reduce 2-DG transport ($P < 0.05$), although to a lesser extent.

The expression of zfGLUT2 in the zebrafish intestine is regulated by the nutritional status. To study the nutritional regulation of zfGLUT2 expression, we examined the effects of

Table 2. *Exon–intron organization of the zebrafish GLUT2 gene*

Exon No.	Exon Size (bp)	Sequence at Exon-Intron Junction				
			5′-Splice Donor	Intron Size (bp)	3′-Splice Acceptor	
1	33	GAG AAG	gtaaattgat	3107	tgtctggcag	CAG TTA
2	96	CAG AAG	gtcactcatc	155	tgtgttatag	GTC ATT
3	200	GGA AG	gtggagtatct	1385	attttgcag	G ATC
4	125	TGT G	gtaagaagaaa	1223	gtgctgcag	GT CTG
5	116	AGT CAA	gtgagtgcca	2463	ttgtctgcag	GTC ATT
6	163	AAG A	gtatgtgcca	3301	tttctgctag	GT CTG
7	188	AAT GCG	gtacgctcat	2656	ctccctttag	ATC TTT
8	105	GTG TCG	gtaaacaggc	1526	gcatgtgtag	GTG TTG
9	102	TTT CAA	gtatgaatcg	629	tgcctctcag	GGC GCT
10	204	TTA GTG	gtaaattgac	1909	tgttccttag	AGT CTC
11	807	CAT TAA	gcttcaagtg			

Exon and intron sequences are indicated in upper and lower-case letters, respectively. The size of exons and introns are given in base pairs (bp).

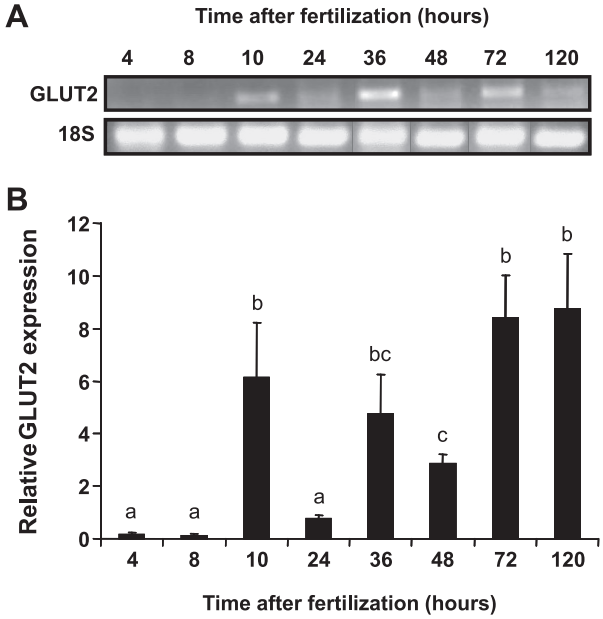

Fig. 4. Developmental expression pattern of zfGLUT2 in zebrafish. Zebrafish embryos were analyzed for zfGLUT2 expression from the early embryonic to the larval stage by RT-PCR (*A*) and quantitative real-time RT-PCR (*B*). Expression levels of zfGLUT2 were normalized to 18S rRNA and in *B*, results are shown as means ± SE relative to the 24 h postfertilization (hpf) stage, which was set to 1. Time after fertilization in zebrafish embryos (until hatching) is given in hours (hpf). The presence of different letters on the bars indicates statistically significant differences between developmental stages ($P < 0.05$).

fasting and refeeding on zfGLUT2 expression in the intestine. Zebrafish were fasted for 15 days and thereafter refed for 6 days. We measured plasma glucose levels to assess the effectiveness of the nutritional experiment. As expected, fasting caused a significant ($P < 0.05$) decrease in plasma glucose levels, compared with the control (fed) state, and refeeding reestablished plasma glucose to control levels (Fig. 9*A*). There was no significant difference in fish length or weight among the fed, fasted, and refed groups (data not shown).

Expression of zfGLUT2 in the zebrafish intestine was assessed by conventional RT-PCR and quantitative real-time PCR (Fig. 9*B*). In fasted fish, zfGLUT2 mRNA levels were higher than those in control fed fish, although the difference was not significant. However, when fasted fish were refed, zfGLUT2 mRNA levels decreased significantly ($P < 0.05$) compared with fasted levels, reaching expression values similar to those found in control fed fish.

DISCUSSION

In mammals, GLUT2 is a low-affinity sugar transporter that plays an important physiological role in the regulation of circulating glucose levels and in glucose sensing (41, 45). In the present study, we have identified a GLUT2 ortholog in zebrafish and described its expression pattern throughout early development and in the adult tissues. In addition, we have characterized its sugar transport properties and studied the nutritional regulation of its mRNA levels in the intestine.

From an evolutionary perspective, it is interesting to note that the gene structure of GLUT2 has been remarkably well conserved between fish and mammals. Similarly to the human GLUT2 gene, the zfGLUT2 gene is composed of 11 exons and, like the mouse and human GLUT2 genes, has the initiation codon in exon 1; however, unlike the rat and human GLUT2 genes, the zfGLUT2 gene has only one exon 4 (1, 36, 47). Furthermore, the immediate genomic region surrounding the GLUT2 gene is also extremely well conserved between zebrafish and humans. The deduced amino acid sequence of zfGLUT2 also contains structural characteristics of GLUT2 (18), suggesting that GLUT2 may have incorporated protein motifs conferring specific transport characteristics early during vertebrate evolution. zfGLUT2, like mammalian GLUT2 and unlike the other class I GLUTs, shows a low conservation of proline residues in TM domain 6, which appears to be important for the glucose transport activity of GLUT2 (50). Moreover, zfGLUT2 also lacks the QLS motif in TM 7 that in mammals is believed to confer the ability to transport fructose with low affinity and glucosamine with high affinity (44, 45). The H(V/M)A motif, which in mammalian GLUT2 substitutes the QLS motif, is not conserved in zfGLUT2, nor in the other fish or avian GLUT2 protein sequences. However, we demonstrate in this study that zfGLUT2 is able to transport glucose, as well as fructose and other sugars similarly to mammalian GLUT2 (see below). In addition to the strong conservation at the protein level between zfGLUT2 and mammalian GLUT2 (i.e., ~60% identical), the conserved synteny of the zfGLUT2 and human GLUT2 genes and the phylogenetic relationship of the deduced zfGLUT2 protein sequence to other vertebrate GLUT2 protein sequences clearly indicate that zfGLUT2 is an ortholog of human GLUT2.

By examining the sugar transport properties of zfGLUT2, we have demonstrated that the affinity constant (K_m) for 2-DG of this transporter, when expressed in *Xenopus* oocytes, is 11 mM. The K_m value for zfGLUT2 is very similar to the values previously obtained for mammalian GLUT2 (from 11.2 to 16.2 mM) under similar experimental conditions (6, 9, 46) but higher than those reported for the other two fish glucose transporters expressed in the same system and calculated by the zero-*trans* method: coho salmon GLUT4 [from 5.03 to 9.68 mM; (7)] and rainbow trout GLUT1 [from 8.3 to 14.9 mM; (37)]. These results are consistent with the notion that GLUT2 is a low-affinity, high-capacity glucose transporter (45). Furthermore, the substrate specificity of zfGLUT2 is similar to that of mammalian GLUT2 (6, 9, 13, 46), allowing the transport of D-glucose, D-mannose, and D-fructose, as well as D-galactose, although to a much lesser extent. Interestingly, zfGLUT2 also appeared to be able to transport L-glucose, albeit with low affinity, similar to what was observed with mammalian GLUT2 (9). Therefore, the basic sugar transport properties of GLUT2 have been strongly conserved between fish and mammals.

The pattern of expression of zfGLUT2 during early zebrafish development observed in this study indicates that zfGLUT2 mRNA is first detected at significant levels throughout the whole embryo at 10 hpf, coinciding with the end of gastrulation. Subsequently, zfGLUT2 expression levels in the whole embryo decrease at 24 hpf, when zfGLUT2 transcripts are clearly observed in the YSL, suggesting a role for zfGLUT2 in sugar transport from maternally derived yolk stores to the developing embryo. Whole embryo zfGLUT2 expression levels increase again significantly at 36 hpf, remaining high until 5 dpf. Interestingly, at 36 hpf is when the liver and the pancreas, two tissues involved in glucose homeostasis and in

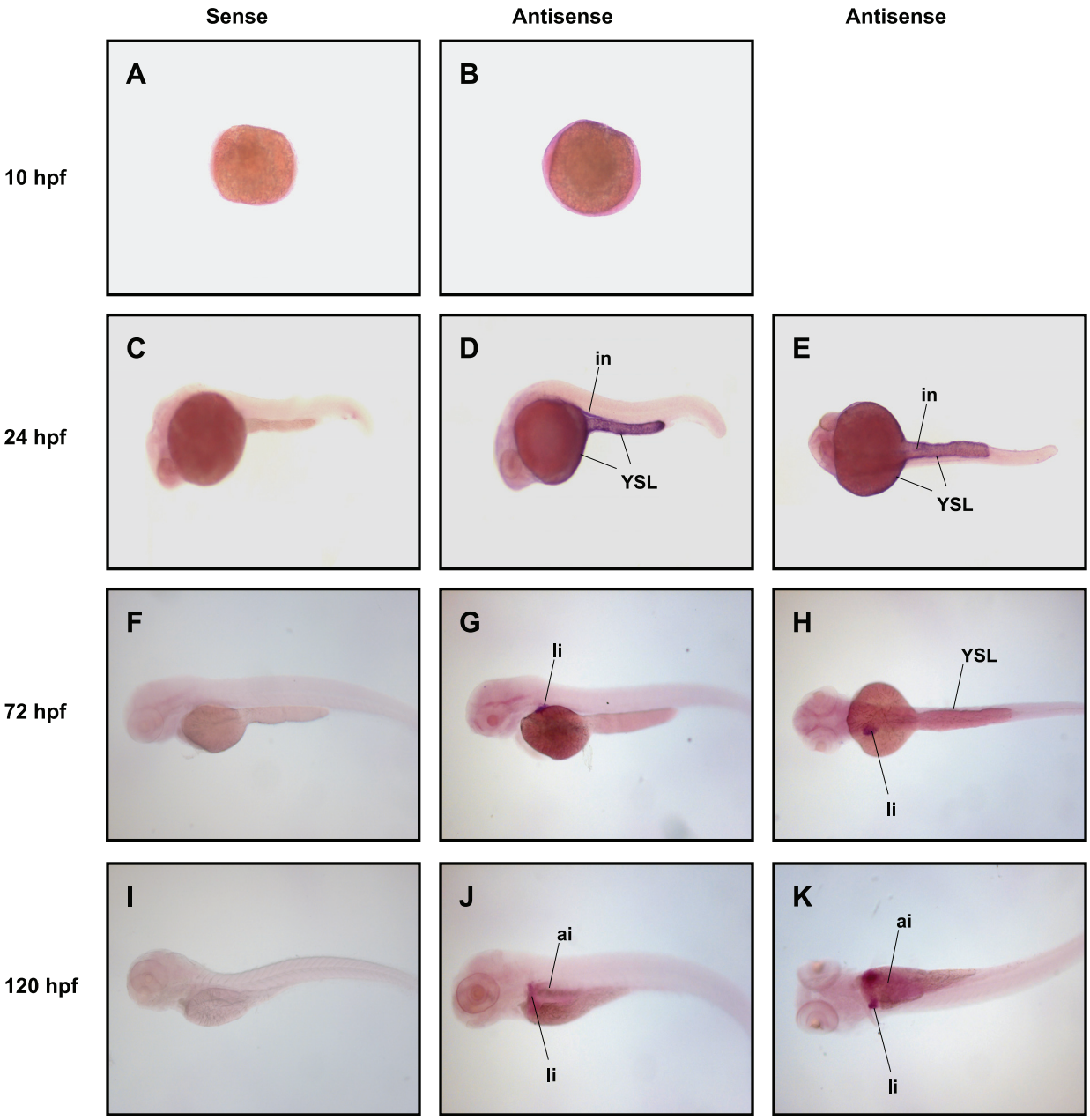

Fig. 5. Whole-mount in situ hybridization analysis of zfGLUT2 during zebrafish embryogenesis and early development. Embryos were hybridized with zfGLUT2 antisense or sense probes. The time after fertilization in zebrafish embryos (until hatching) is given in hours (hpf). Lateral views are shown (*left* and *middle*), and dorsal view (*right*) with the anterior side to the left. Negative controls with the sense-strand probe gave no signal. YSL, yolk syncytial layer; in, intestine; li, liver; ai, anterior intestine.

which GLUT2 has an important functional role in the adult, are undergoing major morphological and functional changes. At this stage, the liver is developing and the endocrine pancreas is already formed and expressing pancreatic hormones such as insulin, glucagon, and somatostatin (5, 29). Furthermore, at this same stage the gut tube formation has just been completed, initiating the process that will result in the formation of a functional intestine ready for the onset of exogenous feeding at ~5 dpf (48). The presence of zfGLUT2 transcripts in liver and intestine at 72 hpf and thereafter is similar to the expression pattern of transferrin and intestinal fatty acid binding protein (IFABP), two carrier proteins and developmental markers for liver and intestine, respectively (28). Like zfGLUT2, transferrin and IFABP are first expressed in the YSL before organogenesis, contributing to the transport of iron and fatty acids to the embryo (28). In later developmental stages, transferrin and IFABP are expressed in a more restricted manner in liver and intestine, respectively (28). Overall, the temporal pattern of expression of zfGLUT2 in the whole embryo, as assessed by real-time PCR, is similar to and confirms that published recently by Tseng et al. (43). However, in contrast to our ISH results, Tseng et al. (43) failed to report expression of GLUT2 in the liver of zebrafish larvae at 72 hpf. In the rainbow trout and the Atlantic cod (15, 22), GLUT2 is also expressed prior to

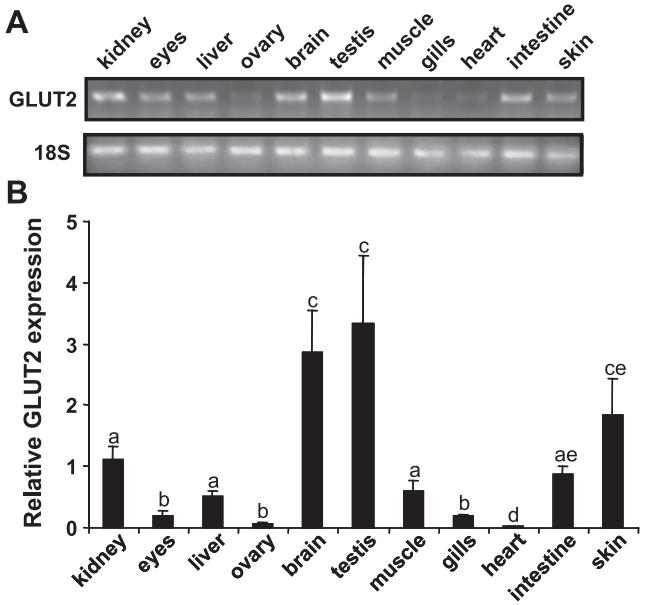

Fig. 6. Tissue expression pattern of zfGLUT2 in adult zebrafish. Tissues from fed adult zebrafish were analyzed for zfGLUT2 expression by RT-PCR (*A*) and quantitative real time PCR (*B*). Expression levels of zfGLUT2 in tissues were normalized to 18S rRNA, and in *B*, results are shown as means ± SE relative to the intestine, which was set to 1. The presence of different letters on the bars indicates statistically significant differences between tissues ($P < 0.05$).

hatching, although no stage-specific or localization information has been reported.

In the adult zebrafish, GLUT2 is expressed in tissues in which this transporter is known to play an important functional role in glucose homeostasis in mammals, namely the liver, intestine, and kidney (45). As expected, zfGLUT2 expression was localized in hepatic cells and in the absorptive cells of the intestine, in which zfGLUT2 may contribute to the entry of sugars from the lumen of the gut. Interestingly, zfGLUT2 was highly expressed in the brain and testis. Although there is no information regarding the possible role of GLUT2 in the testis, the predominance of zfGLUT2 expression in the zebrafish testis over that in the ovary could be related to a possible requirement of glucose as an energy substrate for spermatozoa. GLUT2 is also known to be expressed in the mammalian brain, where it has been postulated to be expressed in glucose-sensing areas involved specifically in glucose and, in more general terms, in energy homeostasis (41). In fish, GLUT2 has been shown to be expressed in the brain of rainbow trout (30, 31) but not in the Atlantic cod (15). Therefore, although we repeatedly failed to observe it by ISH (probably either due to altered mRNA integrity in brain samples throughout the procedure or to a low abundance of transcripts in the brain areas examined), it is tempting to speculate that the expression of zfGLUT2 in the zebrafish brain could be suggestive of the existence of a brain-glucosensing unit, such as that described in mammals (41) and, more recently, in rainbow trout (31, 32). However, the presence of GLUT2, as well as GLUT1 (17), in the zebrafish brain could also be suggestive of a role of glucose transporters in the delivery of glucose as fuel to brain cells. Unfortunately, we were not able to determine whether zfGLUT2 was expressed in the pancreas, a tissue in which GLUT2 plays an important role in the glucose-dependent secretion of insulin (45). Throughout zebrafish's early development, we could not distinguish the labeling by ISH in the

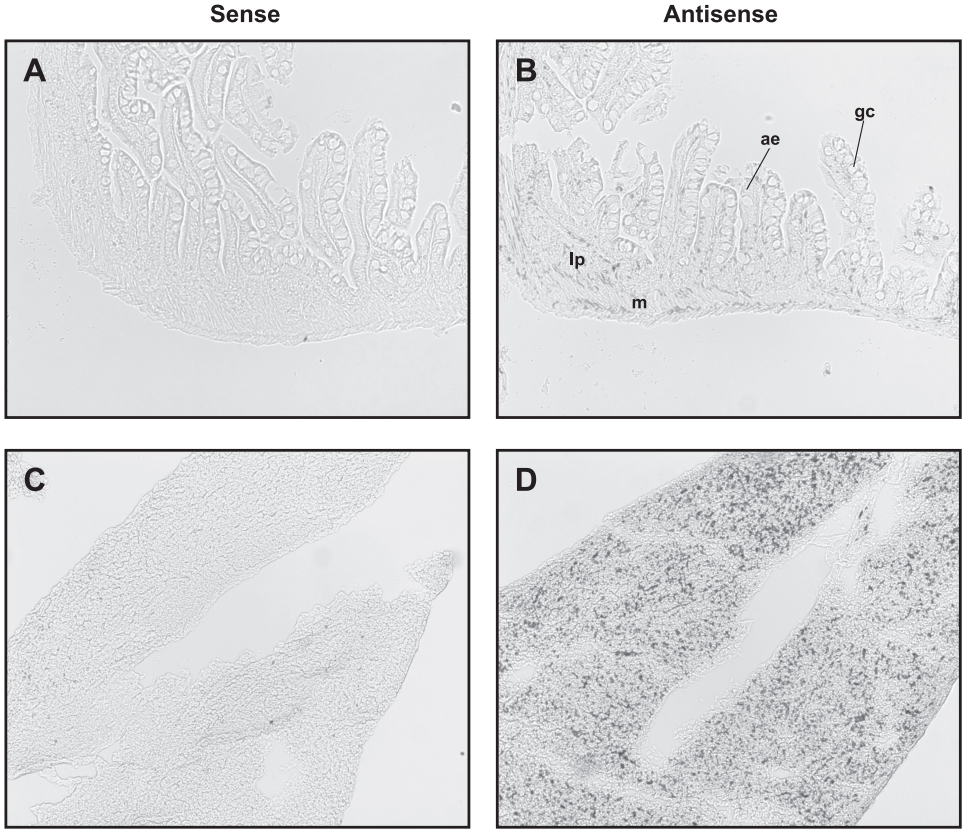

Fig. 7. Detection of zfGLUT2 transcripts by in situ hybridization on frozen sections of adult zebrafish tissues. Sections of intestine (*A* and *B*) and liver (*C* and *D*) were hybridized with zfGLUT2 antisense (*B* and *D*) or sense (*A* and *C*) probes. ae, absorptive enterocyte; gc, goblet cell; lp, lamina propria; m, muscularis layer. Negative controls with the sense-strand probe gave no signal.

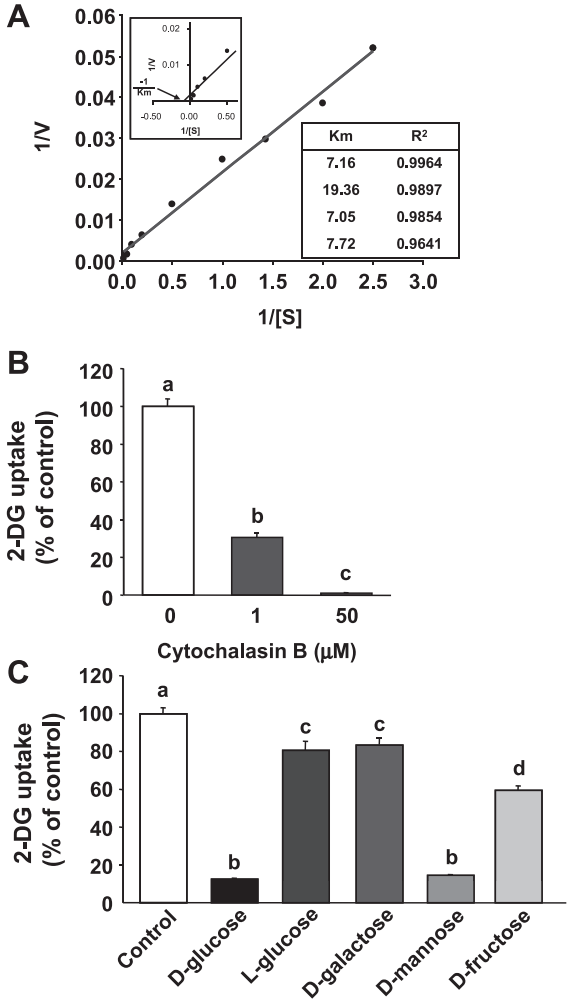

Fig. 8. Functional characterization of zfGLUT2 in *Xenopus* oocytes. *A*: kinetic analysis of glucose uptake in *Xenopus* oocytes expressing zfGLUT2. Lineweaver-Burk plot from the linearization of all of the zero-*trans* kinetics experiments performed combined. *Top inset*: a close-up of the Lineweaver-Burk plot for the higher substrate concentrations used in the experiments showing the point at which the line crosses the *x*-axis, which represents the K_m value. *Bottom inset*: calculated K_m values ($-1/X$ intercept) from the Lineweaver-Burk linearization of four independent experiments (n = 7–10 oocytes per condition in each) calculated separately. The K_m value obtained for the combined plot was 11 mM (R^2 = 0.9901) and the V_{max} value (1/Y intercept) was 556 pmol·oocyte^{-1}·min^{-1}. *B*: inhibition of 2-DG uptake (50 μM, 30 min) in zfGLUT2-expressing oocytes by cytochalasin B. *C*: substrate specificity of the zfGLUT2 transporter as analyzed by competition of 2-DG uptake (50 μM, 30 min) in zfGLUT2-expressing oocytes by D-glucose, L-glucose, D-mannose, D-galactose, and D-fructose (50 mM, final concentration). Specific glucose uptake by zfGLUT2 was calculated by subtracting the uptake value obtained in uninjected oocytes. *B* and *C*: data are expressed as a percentage over the control value (2-DG uptake without competitor or inhibitor, 100%; 3.35 ± 0.29 pmol·min^{-1}·oocyte^{-1}) from two to three independent experiments (8 to 10 oocytes per group). Letters above the bars that differ from one another indicate statistically significant differences between groups ($P < 0.05$).

intestinal tract from that possibly originating from the pancreas, and in the adult, we were unable to identify the tissue. In the future, it will be important to determine the presence of GLUT2 in the zebrafish pancreas and to study its role in mediating the entry of glucose into this tissue.

In this study, we have provided evidence, for the first time in nonmammalian vertebrates, of the nutritional regulation of GLUT2 expression in the zebrafish intestine. The significant decrease in the intestinal expression of zfGLUT2 by refeeding, concomitant with a significant increase in glucose plasma levels, are suggestive of an inverse relationship between glucose plasma levels and zfGLUT2 expression in this tissue. In contrast, fasting has been reported to decrease GLUT2 mRNA and protein levels and refeeding to reverse this effect in rats (14). At this point ,we do not know whether the differences in the response of GLUT2 mRNA expression to fasting and refeeding in the intestine between these two studies can be explained by differences in the regulation of the GLUT2 gene by nutritional factors between zebrafish and rat or to other differences (i.e., methodological, procedural, level of regulation). Specifically, differences in the daily rhythms of intestinal GLUT2 expression could account for differences in the response of GLUT2 expression to fasting and refeeding among different species. Although no information is available in zebrafish, GLUT2 expression and function are known to be under the control of a daily rhythm in mice (11). Unfortunately, the lack of cross-reactivity of antibodies against mammalian GLUT2 (data not shown) prevents us from analyzing changes in zfGLUT2 protein expression until specific antibodies are generated. In addition to changes in expression, dietary glucose induces the transient insertion of GLUT2 into the apical mem-

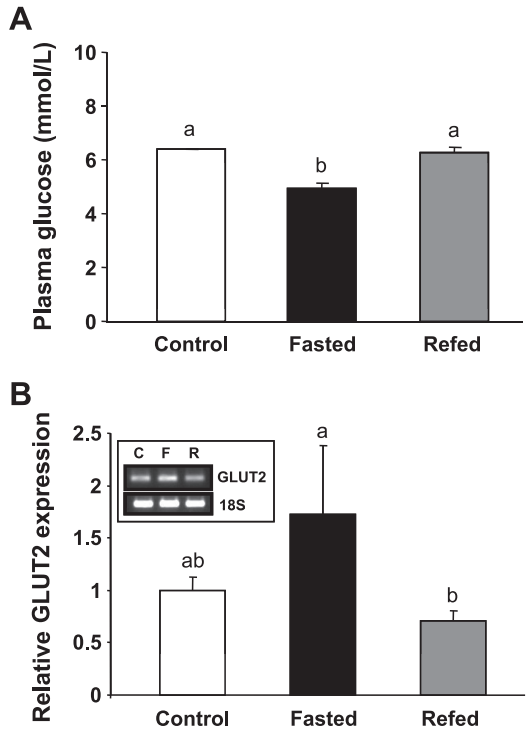

Fig. 9. Effects of fasting and refeeding on intestinal zfGLUT2 expression in zebrafish. Adult zebrafish were fed (C) or starved (F) for 15 days. Starved fish were then refed (R) for 6 days. Plasma glucose levels were measured in control (fed), fasted, and refed fish, and results are shown as means ± SE of three replicate glucose determinations (n = 3) from a pooled plasma sample from each group of fish (*A*). Expression of zfGLUT2 in the intestine of control, fasted, and refed fish was analyzed by RT-PCR (*inset* in *B*) and quantitative real time PCR (*B*). Expression levels of zfGLUT2 in the intestine were normalized to 18S rRNA and in *B*) results are shown as means ± SE relative to the control group, which was set to 1 (n = 6 for each of the fed, starved, and refed groups). Letters above the bars that differ from one another indicate statistically significant differences between groups ($P < 0.05$).

brane of mammalian intestinal cells to increase sugar uptake (20). The glucose-induced insertion of apical GLUT2 is rapid, is associated with activation of the PKC βII subunit and is dependent on the increase in intracellular Ca^{2+}, which is responsible for enterocyte cytoskeletal rearrangement (20). In view of the structural and functional similarities between zfGLUT2 and mammalian GLUT2, we can hypothesize that zfGLUT2 may also possibly contribute to the rapid intestinal glucose absorption by translocating to the apical membrane of enterocytes. Future studies on the specific effects of factors, such as luminal sugars and hormones on the expression and protein localization of GLUT2 in the zebrafish intestine, should be important for our understanding of the regulation of GLUT2.

Perspectives and Significance

From the point of view of the evolution of glucose homeostatic mechanisms and, in particular of glucose transporters, the results from the present study are important because they evidence the remarkable conservation of the structure and functional characteristics of GLUT2 from fish to mammals. Therefore, fish have functionally distinct glucose transporters, as shown for GLUT1 (17, 37), GLUT4 (7, 10) and GLUT2 (this study), which have been conserved during the evolution from fish to mammals. Furthermore, in the context of its recognized interest in metabolic research (35), we set the grounds for the use of zebrafish as a model species for the study of the biology of GLUT2. Future studies on the manipulation of the zfGLUT2 gene in vivo, as well as on the use of functional genomics techniques applied to this species could contribute to our understanding of the physiological role of GLUT2 in glucose homeostasis.

ACKNOWLEDGMENTS

We would like to thank the following persons for their help with in situ hybridization procedures: Adrià Punset and Dr. Florenci Serras (Universitat de Barcelona), Cristina Ruiz and Dr. Anna Bigas (IMIM, Barcelona), and Dr. Pierre-Yves Rescan (SCRIBE-INRA, Rennes, France). We would also like to thank the group of Dr. Enrique Martín-Blanco (Institut de Biologia Molecular de Barcelona) for his help with zebrafish embryo collection and Dr. Josep Rotllant (Instituto de Investigaciones Marinas, CSIC, Vigo) for his help with the comparative genomics analysis.

GRANTS

This study was supported by grants from the Ministerio de Educación y Ciencia, Spain (CSD2007-0002) and the Xarxa de Referència de Recerca i Desenvolupament en Aqüicultura, Generalitat de Catalunya, Spain to J. V. Planas M. Diaz was supported by a fellowship from the Departament d'Universitats, Recerca i Societat de la Informació (Generalitat de Catalunya).

REFERENCES

1. **Ahn YH, Kim JW, Han GS, Lee BG, Kim YS.** Cloning and characterization of rat pancreatic beta-cell/liver type glucose transporter gene: a unique exon/intron organization. *Arch Biochem Biophys* 323: 387–396, 1995.
2. **Alestrom P, Holter JL, Nourizadeh-Lillabadi R.** Zebrafish in functional genomics and aquatic biomedicine. *Trends Biotechnol* 24: 15–21, 2006.
3. **Au A, Gupta A, Schembri P, Cheeseman CI.** Rapid insertion of GLUT2 into the rat jejunal brush-border membrane promoted by glucagon-like peptide 2. *Biochem J* 367: 247–254, 2002.
4. **Baldwin SA.** Mammalian passive glucose transporters: members of an ubiquitous family of active and passive transport proteins. *Biochim Biophys Acta* 1154: 17–49, 1993.
5. **Biemar F, Argenton F, Schmidtke R, Epperlein S, Peers B, Driever W.** Pancreas development in zebrafish: early dispersed appearance of endocrine hormone expressing cells and their convergence to form the definitive islet. *Dev Biol* 230: 189–203, 2001.
6. **Burant CF, Sivitz WI, Fukumoto H, Kayano T, Nagamatsu S, Seino S, Pessin JE, Bell GI.** Mammalian glucose transporters: structure and molecular regulation. *Recent Prog Horm Res* 47: 349–387, 1991.
7. **Capilla E, Diaz M, Albalat A, Navarro I, Pessin JE, Keller K, Planas JV.** Functional characterization of an insulin-responsive glucose transporter (GLUT4) from fish adipose tissue. *Am J Physiol Endocrinol Metab* 287: E348–E357, 2004.
8. **Cheeseman CI.** Intestinal hexose absorption: transcellular or paracellular fluxes. *J Physiol* 544: 336, 2002.
9. **Colville CA, Seatter MJ, Jess TJ, Gould GW, Thomas HM.** Kinetic analysis of the liver-type (GLUT2) and brain-type (GLUT3) glucose transporters in *Xenopus* oocytes: substrate specificities and effects of transport inhibitors. *Biochem J* 290: 701–706, 1993.
10. **Diaz M, Antonescu CN, Capilla E, Klip A, Planas JV.** Fish glucose transporter (GLUT)-4 differs from rat GLUT4 in its traffic characteristics but can translocate to the cell surface in response to insulin in skeletal muscle cells. *Endocrinology* 148: 5248–5257, 2007.
11. **Fatima J, Iqbal CW, Houghton SG, Kasparek MS, Duenes JA, Zheng Y, Sarr MG.** Hexose transporter expression and function in mouse small intestine: role of diurnal rhythm. *J Gastrointest Surg* 13: 634–641, 2009.
12. **Gasteiger E, Gattiker A, Hoogland C, Ivanyi I, Appel RD, Bairoch A.** ExPASy: The proteomics server for in-depth protein knowledge and analysis. *Nucleic Acids Res* 31: 3784–3788, 2003.
13. **Gould GW, Thomas HM, Jess TJ, Bell GI.** Expression of human glucose transporters in *Xenopus* oocytes: kinetic characterization and substrate specificities of the erythrocyte, liver, and brain isoforms. *Biochemistry* 30: 5139–5145, 1991.
14. **Habold C, Foltzer-Jourdainne C, Le Maho Y, Lignot JH, Oudart H.** Intestinal gluconeogenesis and glucose transport according to body fuel availability in rats. *J Physiol* 566: 575–586, 2005.
15. **Hall JR, Short CE, Driedzic WR.** Sequence of Atlantic cod (*Gadus morhua*) GLUT4, GLUT2 and GPDH: Developmental stage expression, tissue expression and relationship to starvation-induced changes in blood glucose. *J Exp Biol* 209: 4490–4502, 2006.
16. **Hall TA.** BioEdit: a user-friendly biological sequence alignment editor and analysis program for Windows 95/98/NT. *Nucl Acids Symp Ser* 41: 95–98, 1999.
17. **Jensen PJ, Gitlin JD, Carayannopoulos MO.** GLUT1 deficiency links nutrient availability and apoptosis during embryonic development. *J Biol Chem* 281: 13382–13387, 2006.
18. **Joost HG, Thorens B.** The extended GLUT-family of sugar/polyol transport facilitators: nomenclature, sequence characteristics, and potential function of its novel members. *Mol Membr Biol* 18: 247–256, 2001.
19. **Kellett GL, Brot-Laroche E.** Apical GLUT2: a major pathway of intestinal sugar absorption. *Diabetes* 54: 3056–3062, 2005.
20. **Kellett GL, Brot-Laroche E, Mace OJ, Leturque A.** Sugar absorption in the intestine: the role of GLUT2. *Annu Rev Nutr* 28: 35–54, 2008.
21. **Kimmel CB, Ballard WW, Kimmel SR, Ullmann B, Schilling TF.** Stages of embryonic development of the zebrafish. *Dev Dyn* 203: 253–310, 1995.
22. **Krasnov A, Teerijoki H, Molsa H.** Rainbow trout (*Onchorhynchus mykiss*) hepatic glucose transporter. *Biochim Biophys Acta* 1520: 174–178, 2001.
23. **Krieg PA, Melton DA.** Functional messenger RNAs are produced by SP6 in vitro transcription of cloned cDNAs. *Nucleic Acids Res* 12: 7057–7070, 1984.
24. **Kumar S, Tamura K, Nei M.** MEGA3: Integrated software for Molecular Evolutionary Genetics Analysis and sequence alignment. *Brief Bioinform* 5: 150–163, 2004.
25. **Lennon G, Auffray C, Polymeropoulos M, Soares MR.** The I.M.A.G.E. Consortium: An Integrated Molecular Analysis of Genomes and their Expression. *Genomics* 33: 151–152, 1996.
26. **Lieschke GJ, Currie PD.** Animal models of human disease: zebrafish swim into view. *Nat Rev Genet* 8: 353–367, 2007.
27. **McGowan KM, Long SD, Pekala PH.** Glucose transporter gene expression: regulation of transcription and mRNA stability. *Pharmacol Ther* 66: 465–505, 1995.
28. **Mudumana SP, Wan H, Singh M, Korzh V, Gong Z.** Expression analyses of zebrafish transferrin, ifabp, and elastaseB mRNAs as differ-

entiation markers for the three major endodermal organs: liver, intestine, and exocrine pancreas. *Dev Dyn* 230: 165–173, 2004.
29. **Ober EA, Field HA, Stainier DYR.** From endoderm formation to liver and pancreas development in zebrafish. *Mech Dev* 120: 5–18, 2003.
30. **Panserat S, Plagnes-Juan E, Kaushik S.** Nutritional regulation and tissue specificity of gene expression for proteins involved in hepatic glucose metabolism in rainbow trout (*Oncorhynchus mykiss*). *J Exp Biol* 204: 2351–2360, 2001.
31. **Polakof S, Miguez JM, Moon TW, Soengas JL.** Evidence for the presence of a glucosensor in hypothalamus, hindbrain, and Brockmann bodies of rainbow trout. *Am J Physiol Regul Integr Comp Physiol* 292: R1657–R1666, 2007.
32. **Polakof S, Miguez JM, Soengas JL.** In vitro evidences for glucosensing capacity and mechanisms in hypothalamus, hindbrain, and Brockmann bodies of rainbow trout. *Am J Physiol Regul Integr Comp Physiol* 293: R1410–R1420, 2007.
33. **Saitou N, Nei M.** The neighbor-joining method: a new method for reconstructing phylogenetic trees. *Mol Biol Evol* 4: 406–425, 1987.
34. **Santos CR, Estevao MD, Fuentes J, Cardoso JC, Fabra M, Passos AL, Detmers FJ, Deen PM, Cerda J, Power DM.** Isolation of a novel aquaglyceroporin from a marine teleost (*Sparus auratus*): function and tissue distribution. *J Exp Biol* 207: 1217–1227, 2004.
35. **Schlegel A, Stainier DY.** Lessons from "lower" organisms: what worms, flies, and zebrafish can teach us about human energy metabolism [Online]. *PLoS Genet* 3: e199, 2007.
36. **Takeda J, Kayano T, Fukomoto H, Bell GI.** Organization of the human GLUT2 (pancreatic beta-cell and hepatocyte) glucose transporter gene. *Diabetes* 42: 773–777, 1993.
37. **Teerijoki H, Krasnov A, Gorodilov Y, Krishna S, Molsa H.** Rainbow trout glucose transporter (OnmyGLUT1): functional assessment in *Xenopus laevis* oocytes and expression in fish embryos. *J Exp Biol* 204: 2667–2673, 2001.
38. **Terova G, Rimoldi S, Brambilla F, Gornati R, Bernardini G, Saroglia M.** In vivo regulation of GLUT2 mRNA in sea bass (*Dicentrarchus labrax*) in response to acute and chronic hypoxia. *Comp Biochem Physiol B Biochem Mol Biol* 152: 306–316, 2009.
39. **Thisse C, Thisse B.** High-resolution in situ hybridization to whole-mount zebrafish embryos. *Nat Protoc* 3: 59–69, 2008.
40. **Thompson JD, Higgins DG, Gibson TJ.** CLUSTAL W: improving the sensitivity of progressive multiple sequence alignment through sequence weighting, position-specific gap penalties and weight matrix choice. *Nucleic Acids Res* 22: 4673–4680, 1994.
41. **Thorens B.** A gene knockout approach in mice to identify glucose sensors controlling glucose homeostasis. *Pflügers Arch* 445: 482–490, 2003.
42. **Thorens B, Sarkar HK, Kaback HR, Lodish HF.** Cloning and functional expression in bacteria of a novel glucose transporter present in liver, intestine, kidney, and beta-pancreatic islet cells. *Cell* 55: 281–290, 1988.
43. **Tseng YC, Chen RD, Lee JR, Liu ST, Lee SJ, Hwang PP.** Specific expression and regulation of glucose transporters in zebrafish ionocytes. *Am J Physiol Regul Integr Comp Physiol* 297: R275–R290, 2009.
44. **Uldry M, Ibberson M, Hosokawa M, Thorens B.** GLUT2 is a high affinity glucosamine transporter. *FEBS Lett* 524: 199–203, 2002.
45. **Uldry M, Thorens B.** The SLC2 family of facilitated hexose and polyol transporters. *Pflügers Arch* 447: 447, 2004.
46. **Vera JC, Rosen OM.** Functional expression of mammalian glucose transporters in *Xenopus laevis* oocytes: evidence for cell-dependent insulin sensitivity. *Mol Cell Biol* 9: 4187–4195, 1989.
47. **Waeber G, Thompson N, Haefliger JA, Nicod P.** Characterization of the murine high K_m glucose transporter GLUT2 gene and its transcriptional regulation by glucose in a differentiated insulin-secreting cell line. *J Biol Chem* 269: 26912–26919, 1994.
48. **Wallace KN, Akhter S, Smith EM, Lorent K, Pack M.** Intestinal growth and differentiation in zebrafish. *Mech Dev* 122: 157–173, 2005.
49. **Wang MY, Tsai MY, Wang C.** Identification of chicken liver glucose transporter. *Arch Biochem Biophys* 310: 172–179, 1994.
50. **Wellner M, Monden I, Mueckler MM, Keller K.** Functional consequences of proline mutations in the putative transmembrane segments 6 and 10 of the glucose transporter GLUT1. *Eur J Biochem* 227: 454–458, 1995.